A Mechanism for the Photochemical Conversion of $FpSi_2Me_5$ to $FpSiMe_3$ (Fp = $(\eta^5\text{-}C_5H_5)Fe(CO)_2$). Infrared Evidence for an Intermediate Iron–Silylene Complex

Anthony Haynes,[†] Michael W. George,[†] Mark T. Haward,[†] Martyn Poliakoff,[†] James J. Turner,*[,†] Neil M. Boag,[‡] and Marjorie Green[‡]

Contribution from the Department of Chemistry, University of Nottingham, Nottingham, NG7 2RD, England, and Department of Chemistry and Applied Chemistry, University of Salford, Salford, M5 4WT, England. *Received March 13, 1990. Revised Manuscript Received October 29, 1990*

Abstract: The photochemistry of the complex $FpSi_2Me_5$ (Fp = $(\eta^5\text{-}C_5H_5)Fe(CO)_2$) is compared to that of $FpSiMe_3$ using a variety of IR spectroscopic techniques. UV photolysis of $FpSi_2Me_5$ in Ar, N_2, or CO matrices leads to CO loss and formation of $CpFe(CO)Si_2Me_5$ (Cp = $(\eta^5\text{-}C_5H_5)$). The equivalent product is not observed on identical treatment of $FpSiMe_3$, but, in N_2 matrices, small quantities of $CpFe(CO)(N_2)SiMe_3$ are generated. Fast time-resolved IR spectroscopy is used to identify primary CO loss photoproducts on flash photolysis of both $FpSi_2Me_5$ and $FpSiMe_3$ in room temperature *n*-heptane solution. Under these conditions, $CpFe(CO)SiMe_3$ reacts rapidly with CO to regenerate $FpSiMe_3$ or with PPh_3 to give $CpFe(CO)(PPh_3)SiMe_3$. By contrast, $CpFe(CO)Si_2Me_5$ is unreactive toward CO or PPh_3 and undergoes an intramolecular decay to give a thermally stable secondary product, X. X is shown to undergo a secondary photochemical reaction with a variety of ligands to give monosilyl products, $CpFe(CO)(L)SiMe_3$ (L = CO, PPh_3, C_2H_4, or N_2). A species with a ν(Si–H) IR band is also produced in each of these reactions. For the reactions of $FpSi_2Me_5$ and $FpSiMe_3$ with N_2, liquid xenon was employed as a cryogenic solvent to stabilize $CpFe(CO)(N_2)SiMe_3$. A mechanism is proposed in which decay of $CpFe(CO)Si_2Me_5$ occurs by intramolecular oxidative addition of the Si–Si bond to the Fe center, giving a thermally stable silyl(silylene) complex, $CpFe(CO)(=SiMe_2)SiMe_3$ (X). Ejection of the $SiMe_2$ fragment from X occurs as a second photochemical step in the deoligomerization. It is suggested that isomerization of the $SiMe_2$ moiety occurs under photochemical conditions, giving a species with Si–H bond(s) and explaining why free silylene fragments have not been trapped in previous studies.

Introduction

The photochemical conversion of a disilanyl–iron complex to the corresponding monosilyl–iron species was first reported in 1974 by Pannell,[1] who observed the deoligomerization of $FpSi_2Me_5$ shown in eq 1 (Fp = $(\eta^5\text{-}C_5H_5)Fe(CO)_2$).

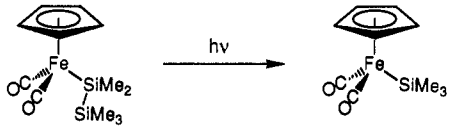

(1)

Recently, there has been considerable interest in the mechanism of this and other closely related photochemical transformations. Pannell reported that photolysis of $FpSiMe_2SiPh_3$ leads to the formation of a mixture of monosilyl–iron complexes[2] (eq 2). Tobita observed a similar reaction for the complex $FpSiMe_2SiMeEt_2$[3] (eq 3).

$$FpSiMe_2SiPh_3 \xrightarrow{h\nu} FpSiPh_3 + FpSiMePh_2 + FpSiMe_2Ph \quad (2)$$

$$FpSiMe_2SiMeEt_2 \xrightarrow{h\nu} FpSiMeEt_2 + FpSiMe_2Et + FpSiMe_3 \quad (3)$$

The product mixtures obtained in these reactions, which are indicative of an intramolecular mechanism, led Pannell and Tobita to propose essentially identical reaction mechanisms. It was suggested that primary photodissociation of CO is followed by migration of an SiR_3 moiety from silicon to iron. This step can be thought of as an oxidative addition of the Si–Si bond to the unsaturated metal center, to give a silyl(silylene)–iron complex (eq 4).

(4)

Subsequent loss of the silylene (SiR_2) moiety and recoordination of CO completes the mechanism. Both Pannell and Tobita employed trapping agents designed to capture free SiR_2 fragments released in the final step of the proposed mechanism but were unable to obtain the expected products from the reaction of the trapping agent with silylene. The observed mixture of products can be explained by rapid scrambling of R groups between silicon atoms in the intermediate species. Further evidence for rapid equilibration of silyl(silylene) intermediates was obtained by Pannell in a study of the product distribution resulting from irradiation of a series of isomeric pairs with the general formula $FpSi_2Ph_{3-n}Me_{2+n}$ (n = 0, 1, 2).[4a] This proposal is also supported by a recent study on the partially deuterated complexes $FpSi_2Me_4(CD_3)$ and $FpSi_2Me_3(CD_3)_2$.[4b]

Silylene complexes have frequently been proposed as intermediates in the reactions of silicon-containing transition-metal systems.[5] However, unlike the analogous, well-known class of carbene compounds, very few silylene complexes have been isolated. The only mononuclear transition-metal complexes known to contain an M=SiR_2 unit have been stabilized by an interaction between the Si atom and the lone pair of electrons of an adjacent Lewis base.[6] There are currently no examples of monomeric silylene complexes existing without base stabilization.

The recent isolation of an intramolecularly base-stabilized photoproduct[7] from an Fp–disilanyl complex gives further evidence

[†] University of Nottingham.
[‡] University of Salford.

(1) Pannell, K. H.; Rice, J. B. *J. Organomet. Chem.* **1974**, *78*, C35.
(2) Pannell, K. H.; Cervantes, J.; Hernandez, C.; Cassias, J.; Vincenti, S. *Organometallics* **1986**, *5*, 1056.
(3) (a) Tobita, H.; Ueno, K.; Ogino, H. *Chem. Lett.* **1986**, 1777. (b) Tobita, H.; Ueno, K.; Ogino, H. *Bull. Chem. Soc. Jpn.* **1988**, *61*, 2797.
(4) (a) Pannell, K. H.; Rozell, J. M.; Hernandez, C. *J. Am. Chem. Soc.* **1989**, *111*, 4482. (b) Ueno, K.; Tobita, H.; Ogino, H. *Chem. Lett.* **1990**, 369.
(5) Aylett, B. J. *Adv. Inorg. Chem. Radiochem.* **1982**, *25*, 1.
(6) (a) Schmid, G.; Welz, E. *Angew. Chem., Int. Ed. Engl.* **1977**, *16*, 785. (b) Straus, D. A.; Tilley, T. D.; Rheingold, A. L.; Geib, S. J. *J. Am. Chem. Soc.* **1987**, *109*, 5872. (c) Zybill, C.; Muller, G. *Organometallics* **1988**, *7*, 1368.
(7) (a) Ueno, K.; Tobita, H.; Ogino, H. *J. Am. Chem. Soc.* **1988**, *110*, 4092. (b) Tobita, H.; Ueno, K.; Shimoi, M.; Ogino, H. *J. Am. Chem. Soc.* **1990**, *112*, 3415.

0002-7863/91/1513-2011$02.50/0

for the deoligomerization mechanisms proposed by Pannell and Tobita. Irradiation of $Fp^*SiMe_2SiMe(OMe)_2$ ($Fp^* = (\eta^5\text{-}C_5Me_5)Fe(CO)_2$) gave a product (A) in which both silicon atoms are bonded to the iron center. Formation of this complex from a primary CO loss photoproduct was explained by the series of reactions shown in eq 5. The silyl(silylene) complex is stabilized by intramolecular electron donation from a methoxy group.

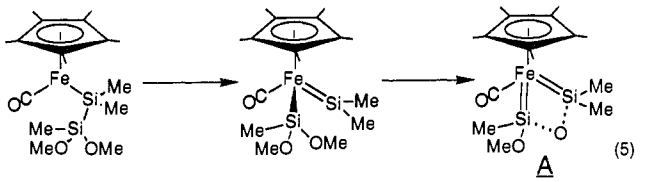

(5)

These observations imply oxidative addition of the Si–Si bond to an unsaturated iron center as a key step. It is likely that a similar process occurs for complexes in which the disilanyl ligand has only alkyl or aryl substituents. However, there is currently no direct evidence for the intermediate silylene complex in these cases.

In this paper, we describe how IR spectroscopy has been used in combination with a variety of techniques to study the photochemistry of silanyl–iron complexes. Reactive photoproducts have been isolated in low-temperature frozen gas matrices for spectroscopic characterization. The behavior of transient species generated by flash photolysis in room temperature solution has been monitored by using fast time-resolved IR (TRIR) spectroscopy. In addition, the photoreactivity of $FpSi_2Me_5$ toward a variety of ligands has been investigated both in conventional room temperature hydrocarbon solvents and in liquid xenon, which provides an ideal cold, inert medium for IR spectroscopic studies. Identical experiments have also been carried out on the closely related monosilyl complex, $FpSiMe_3$, the solution photochemistry of which is well-known.[8-12] These control experiments are designed to reveal the differences caused by extension of the silanyl chain from one to two silicon atoms in length.

Experimental Section

The matrix isolation apparatus, consisting of an Air Products Displex, and a Philips 125-W HPK medium-pressure Hg arc lamp for UV photolysis have been described previously.[13,14] Filters used for photolysis were a $NiSO_4$ (800 g dm^{-3})/$CoSO_4$ (400 g dm^{-3}) aqueous solution (2-cm path length, band pass 230–345 nm), and $\lambda > 300$ nm, $\lambda > 325$ nm, and $\lambda > 400$-nm glass cut-off filters. All IR spectra of matrix isolated species were obtained using a Nicolet 7199 FTIR interferometer and Model 1280 data station (32 K data collect, 256 K Fourier transform, 0.5-cm^{-1} resolution). Matrices were prepared by using the "slow spray-on" technique[14] with the sample in a Pyrex tube attached to the vacuum shroud surrounding the CsBr matrix window. Samples of $FpSi_2Me_5$ were held at room temperature, whereas those of $FpSiMe_3$ were cooled to ca. −10 °C to give the required rate of sublimation onto the matrix window. The rate of deposition of the matrix gas was controlled by using a needle valve. The CsBr matrix window was typically 20 K during deposition of the matrix and cooled to ca. 12 K before photolysis.

The time-resolved IR spectroscopy apparatus[15,16] uses a pulsed UV excimer laser (XeCl, 308 nm) as the source for flash photolysis and a continuous wave CO IR laser to monitor changes in absorption at a particular IR frequency. The CO laser is line-tunable in steps of ca. 4 cm^{-1} between 1700 and 2000 cm^{-1}. Time-resolved IR spectra are built up "point-by-point" by recording IR absorption traces over a range of frequencies.

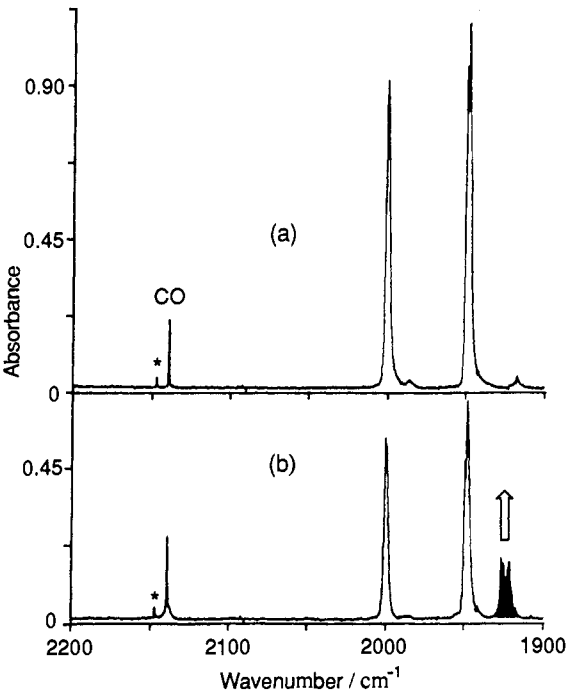

Figure 1. IR spectra illustrating the photochemistry of $FpSi_2Me_5$ isolated in an N_2 matrix at 12 K. (a) Before photolysis (the weak band marked with an asterisk is due to CO coordinated to trace H_2O impurity during deposition[21]). (b) After 230 min near-UV irradiation (>300 nm); the band colored black, due to $CpFe(CO)Si_2Me_5$, is split into two components (see text).

Solutions used in both conventional and flash photolysis experiments were thoroughly degassed by pumping on the solution at room temperature and then placed under an atmosphere of argon or the required reactive gas. Conventional photolysis experiments were carried out in a Pyrex tube. Small portions of the solution were extracted during photolysis in order to monitor reactions by using FTIR spectroscopy. The apparatus for experiments in liquid xenon solution has been described extensively elsewhere.[17,18] At high pressures (20 atm, 300 psi) xenon can be used as a solvent over the temperature range −110 to −30 °C. All solution FTIR spectra were recorded by using a Nicolet MX-3600 or 730 interferometer (16 K data collect, 32 K Fourier transform, 2-cm^{-1} resolution).

Samples of $FpSi_2Me_5$ and $FpSiMe_3$ were prepared by standard literature methods.[8,19] All gases were used without further purification (Ar, N_2, Messer-Griesheim; CO, C_2H_4, BOC research grade). Hydrocarbon solvent (*n*-heptane, Aldrich, HPLC grade) was distilled over CaH_2 under an atmosphere of N_2.

Results and Discussion

Matrix Photochemistry of $FpSi_2Me_5$. Figure 1a shows the infrared spectrum in the terminal C–O stretching region of a sample of $FpSi_2Me_5$ isolated at high dilution in an N_2 matrix at 12 K. The spectrum is essentially identical with that observed for $FpSi_2Me_5$ in alkane solvents,[20] apart from slight shifts and small splittings of bands due to matrix effects. There are two intense absorptions, corresponding to the in-phase and out-of-phase ν(C–O) vibrational modes expected for a nonlinear dicarbonyl structure. The frequencies of the ν(C–O) absorptions of $FpSi_2Me_5$ are compared with those observed in other matrices and *n*-heptane solution in Table I. In addition, there is a weak absorption at 2139

(8) King, R. B.; Pannell, K. H. *Inorg. Chem.* **1968**, *7*, 1510.
(9) Chan, T.-M.; Connolly, J. W.; Hoff, C. D.; Millich, F. *J. Organomet. Chem.* **1978**, *152*, 287.
(10) Cerveau, G.; Chauviere, G.; Colomer, E.; Corriu, R. *J. Organomet. Chem.* **1981**, *210*, 343.
(11) Treichel, P. M.; Komar, D. A. *J. Organomet. Chem.* **1981**, *206*, 77.
(12) Randolph, C. L.; Wrighton, M. S. *J. Am. Chem. Soc.* **1986**, *108*, 3366.
(13) Church, S. P.; Poliakoff, M.; Timney, J. A.; Turner, J. J. *Inorg. Chem.* **1983**, *22*, 3259.
(14) Fletcher, S. C. Ph.D. Thesis, University of Nottingham, 1985.
(15) Poliakoff, M.; Weitz, E. *Adv. Organomet. Chem.* **1986**, *25*, 277.
(16) Dixon, A. J.; Healy, M. A.; Hodges, P. M.; Moore, B. D.; Poliakoff, M.; Simpson, M. B.; Turner, J. J.; West, M. A. *J. Chem. Soc., Faraday Trans. II* **1986**, *82*, 2083.
(17) Maier, W. B.; Poliakoff, M.; Simpson, M. B.; Turner, J. J. *J. Mol. Struct.* **1983**, *80*, 83.
(18) Turner, J. J.; Poliakoff, M.; Howdle, S. M.; Jackson, S. A.; McLaughlin, J. G. *Faraday Discuss. Chem. Soc.* **1989**, *86*, 271.
(19) King, R. B.; Pannell, K. H.; Bennett, C. R.; Ishaq, M. *J. Organomet. Chem.* **1969**, *19*, 327.
(20) Pannell, K. H.; Wu, C. C.; Long, G. J. *J. Organomet. Chem.* **1980**, *186*, 85.

cm^{-1}, indicating the presence of a small amount of uncoordinated CO in the matrix.

The electronic spectrum of $FpSi_2Me_5$ in hydrocarbon solution has been reported previously.[3b] It exhibits two maxima, at 284 and 330 nm, with the low-energy band tailing into the visible region, giving the compound its yellow color. Figure 1b shows the IR spectrum obtained after irradiation of the matrix-isolated sample by using near-UV light (>300 nm). The two ν(C–O) bands of $FpSi_2Me_5$ have decreased in intensity, showing that some of the parent has been destroyed by photolysis. A new absorption (split into two components—see below) has appeared at lower frequency. In addition, the weak absorption at 2139 cm^{-1} has grown, indicating an increase of the amount of free CO in the matrix.

The split photoproduct IR band occurs in the region expected for the ν(C–O) mode of a CO loss product. It is shifted ca. 50 cm^{-1} to low frequency relative to the mean position of the parent ν(C–O) modes. The equivalent shift for the monocarbonyl photoproduct generated from Fp^*SiMe_3 in an alkane matrix[12] is 48 cm^{-1}. These observations suggest that UV photolysis of $FpSi_2Me_5$ causes dissociative loss of CO to give a monocarbonyl photoproduct (eq 6).

$$FpSi_2Me_5 \xrightarrow[N_2/12\ K]{h\nu} CpFe(CO)Si_2Me_5 + CO \qquad (6)$$

Accumulation of a CO loss product, CpFe(CO)R, generally occurs very slowly, if at all in low-temperature matrices, unless the ligand, R, can act as an intramolecular trap for the 16-electron species. For instance, CO loss from FpMe cannot be detected in frozen gas or hydrocarbon glass matrices.[22] Intramolecular trapping can occur via reactions such as β–H transfer (R = C_2H_5[22] or CH_2SiMe_2H[23]) or a change in ligand hapticity (R = η^1-CH_2Ph[24] or η^1-C_5H_5[25]). The ease of formation of a CO loss product from $FpSi_2Me_5$ suggests that the pentamethyldisilanyl ligand is also able to block an empty coordination site. This may simply be due to the steric bulk of the ligand or to a three center electronic interaction.[26]

As noted above, the terminal ν(C–O) absorption of $CpFe(CO)Si_2Me_5$ is split into two major components separated by ca. 5 cm^{-1}. Annealing the matrix to 30 K results in growth of the component at 1927.0 cm^{-1} at the expense of the one at 1921.8 cm^{-1}. This effect is not reversed on cooling the matrix back down to 12 K. However, reversal does occur on subsequent photolysis with visible light (>400 nm). These changes in band shape may be due to site effects in the solid matrix. Alternatively, subtle changes in the structure of the photoproduct may occur, leading to small shifts in ν(C–O). Structural isomerism has previously been proposed for a 16-electron tungsten species. Electronic spectra of $CpW(CO)_2C_2H_5$ obtained in both alkane matrices and room temperature flash photolysis experiments suggest the presence of two species.[27,28] These were assigned as the truly unsaturated complex and an isomer with an agostic interaction between the tungsten atom and a β-hydrogen. A similar pair of isomers may occur in the case of $CpFe(CO)Si_2Me_5$, with one isomer containing a weak interaction between the disilanyl ligand and the iron center. Alternatively, restricted rotation about the Fe–Si bond could result in isomerism. Assuming the vacant coordination site is stereochemically active, two isomers are possible, with the CO group staggered between two methyl groups or between a silyl and a methyl group.

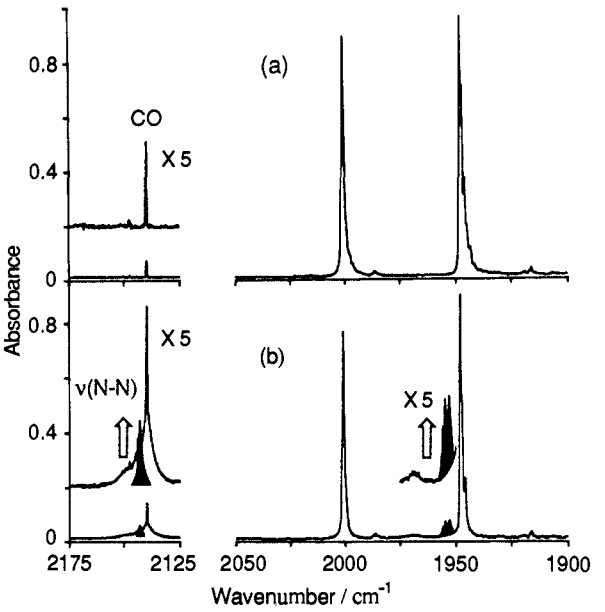

Figure 2. IR spectra illustrating the photochemistry of $FpSiMe_3$ isolated in an N_2 matrix at 12 K: (a) before photolysis and (b) after 15 h UV irradiation (230–345 nm). The bands colored black and shown on an expanded absorbance scale are due to the ν(C–O) and ν(N–N) modes of $CpFe(CO)(N_2)SiMe_3$. The large increase in intensity of the band due to free CO is probably explained by deposition of CO onto the matrix window during long photolysis periods as well as photoejected CO.

Table I. IR Frequencies (cm^{-1}) of Complexes Observed in Low-Temperature Matrices[c]

complex	matrix/solvent			
	Ar	N_2	CO	*n*-heptane[a]
$FpSi_2Me_5$	1949.4, 1950.6	1948.4, 1949.7	1945.0, 1947.7	1946.3
	2001.6, 2002.7	2000.7	1997.6	1997.6
$FpSiMe_3$	1949.4, 1950.6	1945.9, 1947.9		1945.3
	2002.5, 2004.7	2000.8		1998.5
$CpFe(CO)Si_2Me_5$	1928.5	1921.8, 1927.0	1918.9	1924[b]
$CpFe(CO)(N_2)SiMe_3$		1953.0, 1954.9, 1955.8		1952.6
		2142.8		2139.4 ν(N–N)

[a] Error ±0.2 cm^{-1}. [b] Measured by using fast TRIR spectroscopy. [c] Solution data are included for comparison. Components of split bands are bracketed together.

Prolonged photolysis of the matrix using visible light leads to very slow recombination of $CpFe(CO)Si_2Me_5$ with CO to regenerate starting material. Throughout this experiment, no absorptions were observed in the region of the IR spectrum associated with N–N stretching modes. This implies that the N_2 matrix acts as an inert host in this system and does not react with $CpFe(CO)Si_2Me_5$.

The IR spectra obtained on photolysis of $FpSi_2Me_5$ in argon and CO matrices at 12 K indicated that the complex undergoes similar photochemistry under these conditions. The IR frequencies of complexes observed in these experiments are given in Table I. As might be expected, the recombination of $CpFe(CO)Si_2Me_5$ with CO on visible photolysis occurs substantially faster in a pure CO matrix than in Ar or N_2 matrices.

Matrix Photochemistry of $FpSiMe_3$. The photochemistry of $FpSiMe_3$ in frozen gas matrices has not previously been reported.

(21) Dubost, H.; Abouaf-Marguin, L. *Chem. Phys. Lett.* **1972**, *17*, 269.
(22) (a) Kazlauskas, R. J.; Wrighton, M. S. *Organometallics* **1982**, *1*, 602. (b) Mahmoud, K. A.; Rest, A. J.; Alt, H. G. *J. Chem. Soc., Dalton Trans.* **1985**, 1365.
(23) Randolph, C. L.; Wrighton, M. S. *Organometallics* **1987**, *6*, 365.
(24) Blaha, J. P.; Wrighton, M. S. *J. Am. Chem. Soc.* **1985**, *107*, 2694.
(25) Belmont, J. A.; Wrighton, M. S. *Organometallics* **1986**, *5*, 1421.
(26) Crabtree, R. H.; Hamilton, D. G. *Adv. Organomet. Chem.* **1988**, *28*, 299.
(27) (a) Kazlauskas, R. J.; Wrighton, M. S. *J. Am. Chem. Soc.* **1982**, *104*, 6005. (b) Yang, G. K.; Peters, K. S.; Vaida, V. *J. Am. Chem. Soc.* **1986**, *108*, 2511.
(28) Recent matrix and TRIR studies at Nottingham have given further evidence for the existence of two isomers of $CpW(CO)_2C_2H_5$. The truly unsaturated isomer rapidly converts to the β-agostic complex in room temperature solution. Johnson, F. P. A.; Gordon, C. M.; Hodges, P. M.; Poliakoff, M.; Turner, J. J. *J. Chem. Soc., Dalton Trans.*, in press.

Table II. IR Frequencies of Complexes Observed in Solution in *n*-Heptane and Liquid Xenon[b]

complex	*n*-heptane	liquid Xe
$FeSi_2Me_5$	1946.3	1947.7
	1997.6	1999.3
$FpSiMe_3$	1945.3	1946.1
	1998.5	1999.5
$CpFe(CO)Si_2Me_5$	1924[a]	1921.9
$CpFe(CO)SiMe_3$	1928[a]	
X	1943	1944.9
$CpFe(CO)(PPh_3)SiMe_3$	1912.2	
$CpFe(CO)(N_2)SiMe_3$	1952.6	1953.8
	2139.4	2139.5 ν(N–N)
$CpFe(CO)(\eta^2\text{-}C_2H_4)SiMe_3$	1945.6	
$FpCH_2CH_2SiMe_3$	1952.7	
	2006.9	

[a] Measured by using fast TRIR spectroscopy. [b] Error ±0.2 cm^{-1}.

However, irradiation of the analogous pentamethyl species, Fp^*SiMe_3, in an alkane matrix at 77 K is known to result in the slow production of a CO loss photoproduct[12] (ca. 1% conversion after 1 h of photolysis). Interestingly, irradiation (>300 nm) of $FpSiMe_3$, isolated in an argon matrix at 12 K, resulted in no net photochemistry. Even prolonged photolysis using the unfiltered medium pressure Hg arc lamp did not lead to any IR spectral changes.

Figure 2a shows the IR spectrum of $FpSiMe_3$ isolated in an N_2 matrix at 12 K. UV photolysis of the matrix led to extremely slow depletion of the parent ν(C–O) absorptions, even when the unfiltered medium pressure Hg arc lamp was employed. Figure 2b shows the IR spectrum obtained after a total of 17 h of irradiation of the matrix. Loss of parent is accompanied by production of free CO and the growth of two new absorptions, shaded black in Figure 2. The frequencies of bands observed in this experiment are listed in Table I.

The matrix-split absorption centered near 1955 cm^{-1} is assigned as a terminal ν(C–O) mode. The frequency of this band is higher than that predicted for a simple CO loss product, since it is only 19 cm^{-1} lower in frequency than the mean position of the parent ν(C–O) bands. A shift of ca. 50 cm^{-1} is expected for an unsaturated monocarbonyl product (see above).

The other new absorption is very close to the ν(C–O) frequency of matrix-isolated CO. However, the absorption of uncoordinated CO is very narrow in N_2 matrices, and the new absorption shows a significant shift from this band. The new absorption can, however, be assigned as a ν(N–N) mode, since it was not observed in an argon matrix. These results are consistent with the production of species containing both CO and N_2 ligands, as illustrated in eq 7.

$$FpSiMe_3 \xrightarrow[N_2/12\ K]{h\nu} CpFe(CO)(N_2)SiMe_3 + CO \qquad (7)$$

Further evidence for the formation of $CpFe(CO)(N_2)SiMe_3$ was obtained on irradiation of $FpSiMe_3$ in both low-temperature liquid xenon and room temperature hydrocarbon solutions doped with N_2 (see below). The IR spectrum of the dinitrogen complex under these conditions concurs with the matrix assignments (Tables I and II).

The known solution photochemistry of $FpSiMe_3$ is readily explained in terms of efficient primary loss of CO, implying a high quantum yield for this process. However, no absorption attributable to the 16-electron species, $CpFe(CO)SiMe_3$, was observed in argon or N_2 matrices. It is likely that the recombination of the unsaturated species with photoejected CO occurs extremely rapidly within the matrix cage, thus preventing observation of $CpFe(CO)SiMe_3$ under these conditions.

There is, therefore, a marked contrast in the behavior of the monocarbonyl products generated by photolysis of $FpSi_2Me_5$ and $FpSiMe_3$. It appears that the disilanyl ligand of $CpFe(CO)Si_2Me_5$ can block the vacant coordination site at the iron center in a way that is not possible for the monosilyl ligand of $CpFe(CO)SiMe_3$. In this way, the coordinative unsaturation of $CpFe(CO)Si_2Me_5$ is alleviated, preventing rapid combination with CO or N_2.

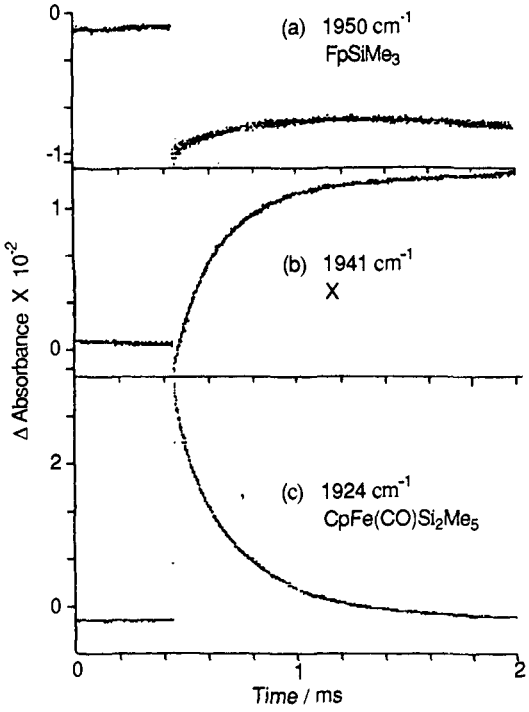

Figure 3. Transient IR absorption traces recorded on flash photolysis (308 nm) of $FpSi_2Me_5$ (2×10^{-3} M) in *n*-heptane at room temperature under argon: (a) 1950 cm^{-1}, depletion of low-frequency parent ν(C–O) band; (b) 1941 cm^{-1}, growth of ν(C–O) band of secondary product, X; and (c) 1924 cm^{-1}, formation and decay of ν(C–O) band of primary photoproduct, $CpFe(CO)Si_2Me_5$.

Flash Photolysis of $FpSi_2Me_5$. Figure 3 shows some of the transient IR absorption traces obtained upon flash photolysis of $FpSi_2Me_5$ in *n*-heptane under an argon atmosphere. The trace recorded at 1950 cm^{-1} (Figure 3a) shows a depletion immediately after the UV pulse, corresponding to the irreversible loss of starting material. (The slight recovery of this absorption after the flash is due to the edge of the absorption of a secondary photoproduct—see below.)

The trace in Figure 3c indicates the formation of a primary photoproduct with an IR absorption near 1924 cm^{-1}. This is close to that assigned to $CpFe(CO)Si_2Me_5$ in low-temperature matrices (Table I) and can reasonably be attributed to the same species. The decay of $CpFe(CO)Si_2Me_5$ in room temperature solution (half-life ca. 200 us) is matched by the generation of a secondary product with an IR absorption near 1941 cm^{-1}, as shown by the trace in Figure 3b. This absorption exhibits no decay even 10 ms after the UV laser pulse, indicating the relative stability of the secondary photoproduct.

Figure 4 shows a series of time-resolved IR spectra obtained during this experiment. Each spectrum is built up point by point from the transient IR absorption measurements made at ca. 4-cm^{-1} intervals. The results are plotted as difference spectra, such that bands due to starting material destroyed by photolysis are negative, whereas photoproducts give rise to positive absorptions. This "stack plot" provides an excellent illustration of the processes observed on flash photolysis of $FpSi_2Me_5$. The primary photoproduct, $CpFe(CO)Si_2Me_5$, decays to give a more stable secondary product, X (eq 8).

$$FpSi_2Me_5 \xrightarrow{h\nu,\ -CO} CpFe(CO)Si_2Me_5 \rightarrow X \qquad (8)$$

The single ν(C–O) absorption band of X suggests that it is also a monocarbonyl species. The conversion of $CpFe(CO)Si_2Me_5$ to X obeys first-order kinetics with a rate constant of 3.5 (±0.2) × 10^3 s^{-1}. The rate of this reaction was found to be independent of the concentrations of both starting material and added CO, within the limits of experimental error. (By contrast, the presence of 2 atm of CO in experiments on $FpSiMe_3$ has a pronounced effect—see below). This is consistent with the production of X

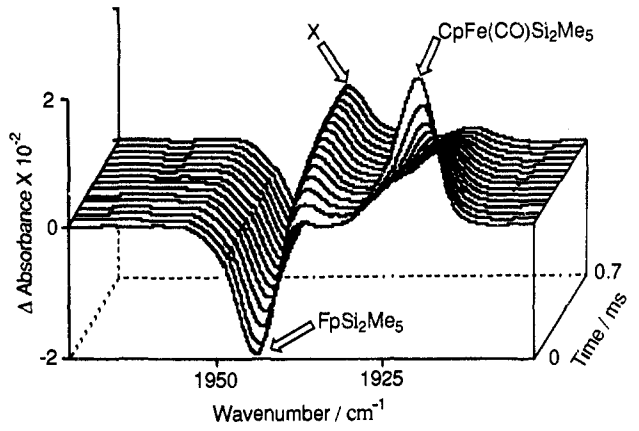

Figure 4. A series of time-resolved IR spectra obtained after flash photolysis (308 nm) of $FpSi_2Me_5$ (2×10^{-3} M) in *n*-heptane at room temperature under argon. The time delay between each spectrum is 50 μs. Bands are labeled according to the species responsible. The high-frequency ν(C–O) band of $FpSi_2Me_5$ lies out of the tuning range of the CO laser.

via an intramolecular reaction of $CpFe(CO)Si_2Me_5$. The same photochemistry was observed when a five times excess of PPh_3 was added to the solution, with no evidence for formation of a substituted product, $CpFe(CO)(PPh_3)Si_2Me_5$, on flash photolysis.

Flash Photolysis of $FpSiMe_3$. Figure 5a shows the IR absorption trace obtained at 1928 cm^{-1} on flash photolysis of a solution of $FpSiMe_3$ in *n*-heptane under an atmosphere of argon. It shows that a transient IR absorption is produced immediately after the UV flash, which then decays rapidly, with a half-life of ca. 9 μs.

The frequency of the single primary photoproduct band is close to that expected for a monocarbonyl species formed by dissociative loss of CO from $FpSiMe_3$. No such photoproduct was observed in low-temperature matrices, suggesting that recombination of $CpFe(CO)SiMe_3$ with CO is a facile process. To probe whether the primary photoproduct observed in solution is indeed a CO loss product, the experiment was repeated with different pressures of CO above the solution.

Figure 5b shows the IR absorption trace obtained at 1928 cm^{-1} after introduction of a pressure of 0.1 atm of CO above the solution. The decay of the transient ν(C–O) band at 1928 cm^{-1} is approximately twice as fast under these conditions (half-life ca. 4 ms). On increasing the pressure of CO to 2 atm, the photoproduct could not be detected, suggesting the occurrence of a very fast back-reaction with CO. These results are consistent with generation of a reactive monocarbonyl photoproduct, which recombines rapidly with CO (eq 9).

$$FpSiMe_3 \xrightarrow[+CO]{h\nu, -CO} CpFe(CO)SiMe_3 \qquad (9)$$

When a five times excess of PPh_3 was present in solution. $CpFe(CO)SiMe_3$ could not be detected on flash photolysis. However, a new long-lived absorption was observed to grow within the lifetime of the IR detector at 1912 cm^{-1}. This is assigned to the stable substituted product, $CpFe(CO)(PPh_3)SiMe_3$,[8] indicating that $CpFe(CO)SiMe_3$ reacts rapidly with PPh_3.

Thus, fast TRIR spectroscopy has shown that the CO loss photoproducts generated by flash photolysis of $FpSi_2Me_5$ or $FpSiMe_3$ exhibit substantially different behavior in solution. Loss of CO from $FpSi_2Me_5$ is irreversible. The results suggest that $CpFe(CO)Si_2Me_5$ undergoes an intramolecular reaction to give a relatively stable secondary product, X. By contrast, $CpFe(CO)SiMe_3$ reacts rapidly with CO to regenerate $FpSiMe_3$ or with PPh_3 to give $CpFe(CO)(PPh_3)SiMe_3$.

Room Temperature Photochemistry Monitored by FTIR Spectroscopy. The room temperature solution photochemistry of both Fp–silanyl complexes was also monitored on a slower time scale by using FTIR spectroscopy. Irradiation (>300 nm) of $FpSiMe_3$ in *n*-heptane under argon results in little net photochemistry. Only ca. 2% of the parent was destroyed by 30-min of photolysis, the only product observed by IR spectroscopy being a small amount of the dinuclear iron complex, Fp_2. When the experiment was repeated under an atmosphere of CO, even prolonged photolysis caused no changes in the IR spectrum. These results are in agreement with the findings from matrix isolation and flash photolysis experiments on $FpSiMe_3$, which implied rapid recombination of $CpFe(CO)SiMe_3$ with CO.

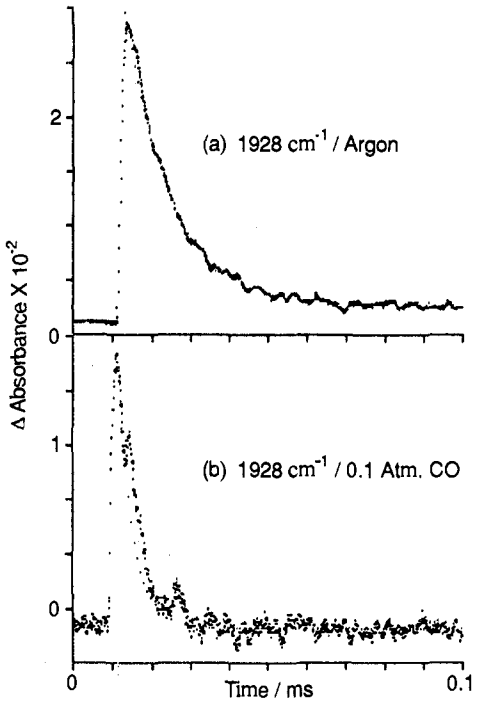

Figure 5. Transient IR absorption traces recorded at 1928 cm^{-1} on flash photolysis (308 nm) of $FpSiMe_3$ (2×10^{-3} M) in *n*-heptane at room temperature: (a) under 2 atm argon and (b) under 0.1 atm CO/1.9 atm argon. Note the increase in decay rate of the absorption due to $CpFe(CO)SiMe_3$ in the presence of added CO.

Figure 6a shows the IR difference spectrum obtained after 60 s of photolysis of $FpSi_2Me_5$ in *n*-heptane under an argon atmosphere. Depletion of the two parent ν(C–O) bands is accompanied by the growth of a single product ν(C–O) absorption. This band coincides with that assigned to the secondary product, X, observed in flash photolysis experiments. (Scaled computer subtraction of the parent bands reveals the peak position of the ν(C–O) band of X to be 1943 cm^{-1}.) No decay of X or regeneration of starting material was observed after 90 min, during which time the solution was left in the dark at room temperature. Thus, the only stable product detected by IR spectroscopy after brief photolysis of $FpSi_2Me_5$ is X. No such intermediate species has been reported in previous studies on the photochemical conversion of $FpSi_2Me_5$ to $FpSiMe_3$.[1-4]

Continued photolysis leads to further conversion of starting material to X. However, the concentration of X reaches a maximum value and then begins to decrease. At the same time, small but significant shifts in the ν(C–O) absorptions of the "parent" are observed, which are consistent with the production of $FpSiMe_3$, as observed by other workers. These results suggest that the intermediate monocarbonyl species, X, is thermally stable but undergoes a secondary photochemical reaction yielding $FpSiMe_3$.

It would be extremely valuable for the identification of X to obtain NMR spectra, particularly ^{29}Si. However the intensity of ν(CO) bands means that IR is much more sensitive than NMR. Moreover X itself is photosensitive, and all attempts, with narrow band filtered UV and even an excimer laser, to generate sufficient X for NMR studies were unsuccessful.

An experiment designed to illustrate this secondary photochemical step was carried out as follows: An *n*-heptane solution of $FpSi_2Me_5$ was initially irradiated under argon, by using filtered

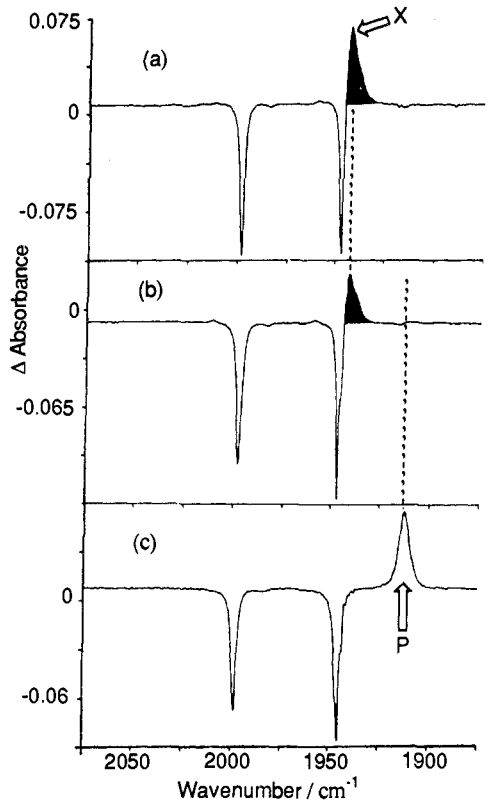

Figure 6. IR difference spectra obtained after 1-min irradiation (>300 nm) of (a) $FpSi_2Me_5$ (1.7×10^{-3} M) in *n*-heptane under argon: (b) $FpSi_2Me_5$ (2.0×10^{-3} M) in *n*-heptane doped with PPh_3 (10^{-2} M); and (c) $FpSiMe_3$ (2.0×10^{-3} M) in *n*-heptane doped with PPh_3 (10^{-2} M). The bands colored black in spectra (a) and (b) are due to X. The band labeled P in spectrum (c) is due to $CpFe(CO)(PPh_3)SiMe_3$. Note the absence of any ν(C–O) band due to a phosphine product on brief photolysis of $FpSi_2Me_5$ (spectrum (b)).

UV light (300–345 nm), in order to minimize secondary photochemical reactions. When the concentration of X reached its maximum value, as judged by IR spectroscopy, the solution was placed under an atmosphere of CO. The intermediate, X, was found to be stable even in the presence of excess CO. The spectra shown in Figure 7a were obtained before and after continued photolysis of the solution by using visible light (>400 nm). These spectra show the depletion of the ν(C–O) band due to X at 1943 cm^{-1}, and the growth of two IR bands, colored black, assigned to $FpSiMe_3$. A difference spectrum illustrating this reaction is shown in Figure 7b. These spectra provide direct evidence that $FpSiMe_3$ is generated via a photoinduced reaction of X with CO. Therefore, there are two distinct photochemical steps in the deoligomerization of $FpSi_2Me_5$, as summarized in eq 10.

$$FpSi_2Me_5 \xrightarrow[-CO]{h\nu} X \xrightarrow[+CO]{h\nu} FpSiMe_3 + \text{"}SiMe_2\text{"} \quad (10)$$

This reaction is accompanied by the growth of a broad, weak IR absorption at 2121 cm^{-1}, shown expanded in Figure 7. (The same band was observed when the reaction was carried out under an argon atmosphere but was not generated on irradiation of $FpSiMe_3$ under any circumstances.) This absorption occurs in the ν(Si–H) region of the IR spectrum and may be due to a silicon-containing species resulting from expulsion of an "$SiMe_2$" fragment from the metal complex. The possible identity of this species will be discussed in more detail later in the paper.

It is well-known that irradiation of $FpSiMe_3$ can lead to substitution of CO by a variety of added ligands.[8-12] In the present study, the solution photochemistry of $FpSi_2Me_5$ in the presence of PPh_3, C_2H_4, or N_2 was compared with that of $FpSiMe_3$ under identical conditions.

Reaction with PPh_3. Figure 6b shows the IR difference spectrum obtained after brief photolysis (>300 nm) of $FpSi_2Me_5$ in *n*-heptane containing a 5-fold excess of PPh_3. It is essentially identical with the difference spectrum shown in Figure 6a, recorded in the absence of phosphine. The ν(C–O) band colored black is assigned to X. There is no absorption which could be assigned to a phosphine-substituted product in the early stages of photolysis. Identical treatment of $FpSiMe_3$ results in loss of parent and growth of an absorption at 1912 cm^{-1}, assigned to $CpFe(CO)(PPh_3)SiMe_3$[8] (Figure 6c).

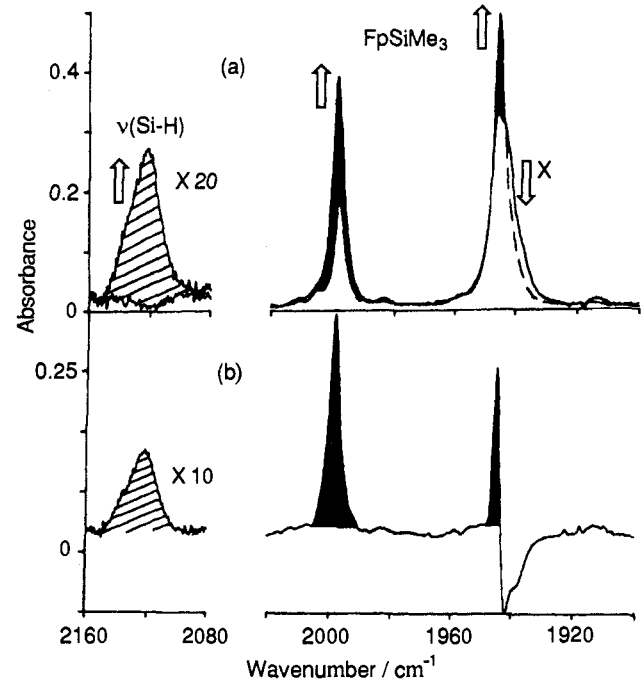

Figure 7. IR spectra illustrating the photochemical reaction of X with CO to give $FpSiMe_3$: (a) starting spectrum obtained after 300 min filtered UV irradiation (230–345 nm) of $FpSi_2Me_5$ in *n*-heptane under argon to generate X. The bands colored black, due to $FpSiMe_3$, were produced after 345 mins further photolysis (>400 nm) under CO. Arrows indicate the behavior of individual bands. (b) Difference spectrum showing depletion of shoulder at 1943 cm^{-1} due to X. Note the cross-shatched ν(Si–H) band produced during this reaction, shown with an expanded absorbance scale.

The spectra in Figure 8a illustrate the clean photochemical reaction of $FpSiMe_3$ to give $CpFe(CO)(PPh_3)SiMe_3$ during continued photolysis. A similar series of spectra, recorded during irradiation of $FpSi_2Me_5$ are displayed in Figure 8b. The ν(C–O) band of X appears as a shoulder, which reaches a maximum intensity and then subsides. At the same time, the growth of two new absorptions is observed, neither of which are apparent in the early stages of photolysis. The intense low-frequency band occurs at exactly the same wavenumber as the ν(C–O) mode of $CpFe(CO)(PPh_3)SiMe_3$. The weaker absorption in the ν(Si–H) region corresponds with the band produced during the photochemical reaction of X with CO to give $FpSiMe_3$ (see above).

These results are consistent with the photochemistry summarized in eq 11. A phosphine-substituted product is only formed after deoligomerization of the silanyl ligand.

$$FpSi_2Me_5 \xrightarrow[-CO]{h\nu} X \xrightarrow[+PPh_3]{h\nu} CpFe(CO)(PPh_3)SiMe_3 + \text{"}SiMe_2\text{"} \quad (11)$$

Reaction with C_2H_4. Entirely analogous photochemistry was observed by using ethylene as the added ligand (eq 12).

$$FpSi_2Me_5 \xrightarrow[-CO]{h\nu} X \xrightarrow[+C_2H_4]{h\nu} CpFe(CO)(C_2H_4)SiMe_3 + \text{"}SiMe_2\text{"} \quad (12)$$

The ethylene complex, $CpFe(CO)(\eta^2\text{-}C_2H_4)SiMe_3$ has previously been observed on irradiation of $FpSiMe_3$ in the presence of ethylene.[12] However, brief photolysis of $FpSi_2Me_5$ under these conditions was found to yield X as the only product. The ethylene

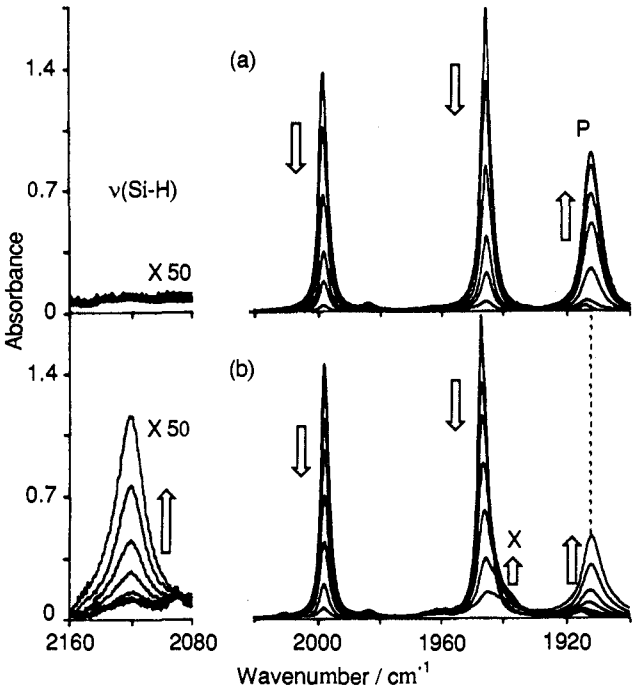

Figure 8. (a) IR spectra recorded during 130-min irradiation (>300 nm) of $FpSiMe_3$ (2.0×10^{-3} M) and PPh_3 (10^{-2} M) in *n*-heptane. The growth of the band labeled P is due to formation of $CpFe(CO)(PPh_3)SiMe_3$. (b) IR spectra recorded during 120-min irradiation (>300 nm) of $FpSi_2Me_5$ (2.0×10^{-3} M) and PPh_3 (10^{-2} M) in *n*-heptane. Note the initial production of a shoulder due to X near 1940 cm^{-1}. The generation of $CpFe(CO)(PPh_3)SiMe_3$ on prolonged photolysis is matched by the growth of a ν(Si–H) band not produced in (a) (shown with an expanded absorbance scale). Arrows indicate the behavior of particular absorptions during photolysis.

complex was only generated after longer photolysis times. This reaction was again accompanied by the growth of an absorption in the ν(Si–H) region at 2121 cm^{-1}. The identity of $CpFe(CO)(\eta^2\text{-}C_2H_4)SiMe_3$ was confirmed by monitoring its thermal reaction with CO, which is known to lead to insertion of ethylene into the Fe–Si bond[12] (eq 13). The IR data for this experiment are given in Table II.

$$CpFe(CO)(\eta^2\text{-}C_2H_4)SiMe_3 \xrightarrow{CO} FpCH_2CH_2SiMe_3 \quad (13)$$

Reaction with N_2. Irradiation of $FpSiMe_3$ in an N_2 matrix gave evidence for formation of the previously unreported dinitrogen complex, $CpFe(CO)(N_2)SiMe_3$. It is of interest whether this coordinatively saturated complex is stable in solution.

Photolysis of a solution of $FpSiMe_3$ in *n*-heptane, under a pressure of 1 atm of N_2 leads to production of small amounts of the dimeric species, Fp_2. In addition, two new IR bands, not observed in the absence of N_2, are produced at 1953 (shoulder) and 2139.4 cm^{-1}. These frequencies correspond well with those assigned to the ν(C–O) and ν(N–N) modes of $CpFe(CO)(N_2)SiMe_3$ in a low-temperature matrix (Table I) and can confidently be assigned to the same species. The N_2 complex can only be generated in small amounts in room temperature solution and is unstable with respect to $FpSiMe_3$ (half-life ca. 20 min under N_2 in the dark). In order to monitor the photochemistry of this system more easily, it is necessary to employ a medium in which the lifetime of the N_2 complex is extended.

The use of liquid xenon as a solvent has recently proved to be a valuable tool in the study of reactive organometallic molecules.[18,29] It is a cold, inert solvent which is completely transparent to IR light. In addition, the cell employed enables a high pressure of gas to be introduced above the solution. Hence, large concentrations of dopants such as N_2 can be dissolved in the solution.

The Fp–silanyl complexes under study dissolve readily in liquid xenon, and it proved to be quite difficult to control the amount of iron complex in solution. Consequently, the ν(C–O) absorptions of the starting material were often very intense, extending off-scale at the start of an experiment. When this was the case, the amount of Fp–silanyl complex in solution was monitored by observing the isotopic satellites due to natural abundance $CpFe(^{12}CO)(^{13}CO)$–silanyl isotopomers.

Near-UV irradiation (>325 nm) of $FpSiMe_3$ in undoped liquid xenon at −100 °C resulted in no net photochemistry. Figure 9a shows the IR spectra recorded before and after 30-min irradiation of the same solution, with a pressure of 150 psi of N_2 added to the cell. Photolysis leads to the growth of two new absorptions at 2139.5 and 1953.8 cm^{-1}, shaded black in Figure 9a. These bands retain the same relative intensities and correspond well with the ν(C–O) and ν(N–N) modes of $CpFe(CO)(N_2)SiMe_3$, in N_2 matrices or room temperature solutions (Tables I and II).

The N_2 complex was found to be thermally stable in liquid xenon at −100 °C, even when the cell was pressurized with CO. However, irradiation of the solution containing $CpFe(CO)(N_2)SiMe_3$ with an overpressure of 15 psi of CO resulted in the reverse photochemical reaction, regenerating $FpSiMe_3$. This photochemistry is summarized in eq 14.

$$FpSiMe_3 \underset{h\nu,\,-N_2}{\overset{h\nu,\,+N_2}{\rightleftharpoons}} CpFe(CO)(N_2)SiMe_3 + CO \quad (14)$$

Figure 9b shows the IR spectra obtained during irradiation (>325 nm) of $FpSi_2Me_5$ in undoped liquid xenon solution at −100 °C. Photolysis leads to loss of starting material and the appearance of two photoproduct ν(C–O) absorptions. The weak band at 1921.9 cm^{-1} is close to the absorption of $CpFe(CO)Si_2Me_5$, the primary photoproduct observed in matrix isolation and flash photolysis experiments. The other new ν(C–O) absorption appears initially as a shoulder on the low-frequency parent band, but, after prolonged photolysis, it is resolved as a separate peak at 1944.9 cm^{-1}. Allowing for a solvent frequency shift, this band is assigned to X, observed in hydrocarbon solvents at room temperature.

The growth of a broad absorption at 2121 cm^{-1} in Figure 9b suggests that a species with Si–H bond(s) is again generated. This indicates that the secondary photochemical reaction (i.e., conversion of X to $FpSiMe_3$) occurs under these conditions. However, the ν(C–O) bands of $FpSiMe_3$ cannot be distinguished from those of remaining $FpSi_2Me_5$ in these spectra.

The experiment was repeated with an overpressure of 150 psi N_2 in the cell. The IR spectra obtained during photolysis (Figure 9c) are very similar to those recorded in the absence of N_2. However, an additional weak, narrow feature is apparent at 2139.5 cm^{-1}, which coincides with the ν(N–N) band of $CpFe(CO)(N_2)SiMe_3$, generated from $FpSiMe_3$ in liquid xenon (Figure 9a). The yield of $CpFe(CO)(N_2)SiMe_3$ is much smaller than that generated from $FpSiMe_3$ after comparable photolysis times, which is consistent with its formation via two photochemical steps (eq 15).

$$FpSi_2Me_5 \xrightarrow{h\nu,\,-CO} X \xrightarrow{h\nu,\,+N_2} CpFe(CO)(N_2)SiMe_3 + \text{"}SiMe_2\text{"} \quad (15)$$

Hence, the relative photoreactivity of $FpSi_2Me_5$ and $FpSiMe_3$ toward N_2 in liquid xenon solution is very similar to that observed at room temperature for added ligands such as PPh_3 or C_2H_4.

A Mechanism for the Deoligomerization of $FpSi_2Me_5$. The results described above can be explained by the mechanism shown in Scheme I. This mechanism is similar to those previously put forward by Pannell[2] and Tobita,[3] except that two distinct photochemical steps are involved.

The primary photochemical process for both $FpSiMe_3$ and $FpSi_2Me_5$ has been confirmed as dissociative loss of CO. However, the coordinatively unsaturated species produced by these reactions behave in substantially different manners. $CpFe(CO)SiMe_3$ reacts rapidly with a variety of ligands to give $CpFe(CO)(L)SiMe_3$ (L = CO, N_2, PPh_3 and C_2H_4). By contrast, $CpFe(CO)Si_2Me_5$ is

(29) Turner, J. J.; Healy, M. A.; Poliakoff, M. In *High Energy Processes in Organometallic Chemistry*; Suslick, K., Ed.; ACS Symposium Series, 333; 1987; Chapter 7.

Scheme I. A Mechanism for the Photochemical Reactions of $FpSi_2Me_5$ and $FpSiMe_3$

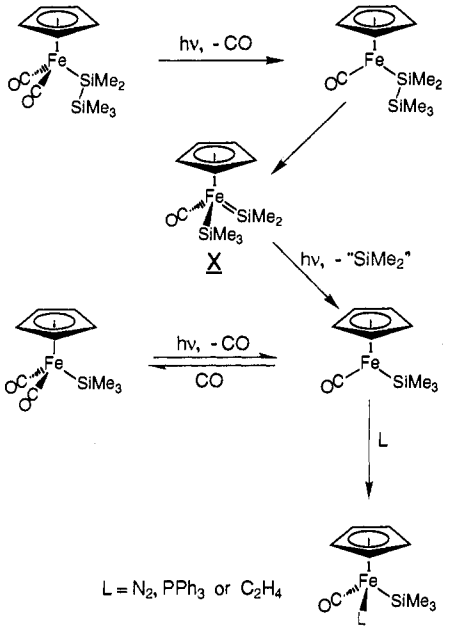

unreactive toward potential ligands and undergoes an intramolecular reaction to give X (except in frozen gas matrices). It is proposed that X is a silyl(silylene)–iron complex resulting from intramolecular oxidative addition of the Si–Si bond. X is thermally stable in room temperature solution but reacts with potential ligands under photochemical conditions to give $CpFe(CO)(L)SiMe_3$ (L = CO, N_2, PPh_3, and C_2H_4). Since the same products are generated photochemically from both $FpSiMe_3$ and X, it is proposed that a common intermediate is involved, namely $CpFe(CO)SiMe_3$. Therefore the second photochemical step must involve loss of an $SiMe_2$ fragment.

The important features of the mechanism will now be discussed. It is possible to rationalize the lack of reactivity displayed by $CpFe(CO)Si_2Me_5$ toward potential ligands in terms of an interaction between the disilanyl ligand and the 16-electron iron center. Several three-center interactions[26] can be envisaged in which a covalent σ-bond of the disilanyl ligand is considered to act as a ligand at the iron center. Three possible structures of this type are illustrated below. Interactions involving an α-Si–CH_3 unit are not considered, since $CpFe(CO)SiMe_3$ does not exhibit similar stabilization.

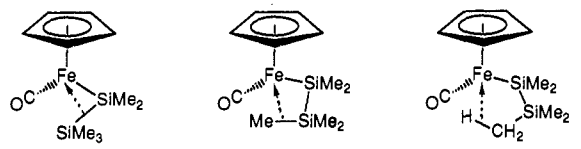

(1) (2) (3)

Each of these structures can be regarded as an intermediate stage in the intramolecular oxidative addition of the respective covalent bond. Irradiation of $FpSi_2Me_5$ leads ultimately to deoligomerization (eq 1), which requires cleavage of the Si–Si bond. Therefore it is tempting to speculate that $CpFe(CO)Si_2Me_5$ is stabilized by an interaction like that shown in structure **1**. It is worth noting that the Si–Si bonds of permethylpolysilanes can form charge-transfer complexes with *n*-acceptors such as tetracyanoethylene (TCNE), in which electron density is donated from a Si–Si σ-bond to the acceptor molecule.[30] This property of Si–Si bonds may be related to the ability of a disilanyl ligand to interact with an unsaturated metal center. It was noted earlier that in low-temperature matrices, $CpFe(CO)Si_2Me$ reacts slowly with CO when irradiated with visible light. Excitation in this manner may open up the coordination site blocked by the disilanyl ligand, enabling recombination with CO.

The shift of ν(C–O) to higher frequency on formation of X from $CpFe(CO)Si_2Me_5$ is consistent with an oxidative addition reaction. Such reactions involving Si–C cleavage or γ-H transfer are not generally observed. By contrast, the reactivity of Si–Si bonds toward transition-metal complexes is well-known.[5] Oxidative addition of the Si–Si bond of $CpFe(CO)Si_2Me_5$ to the Fe center (eq 4) would result in a silyl(silylene)–iron complex, previously suggested as an intermediate by Pannell and Tobita.[2,3] The recent isolation of an intramolecularly base-stabilized bis(silylene) complex, on irradiation of $Fp^*SiMe_2SiMe(OMe)_2$, gives further evidence for this proposal.[4] The observed thermal stability of X may also explain why mixtures of products were observed for $FpSiMe_2SiPh_3$[2] and $FpSiMe_2SiMeEt_2$.[3] There would clearly be sufficient time for alkyl migration to occur, although there is no further evidence as to the mechanism of this process.

An analogy can be drawn between Si–Si bond activation and C–H activation. Molecular orbital calculations indicate that oxidative addition of an R–H bond (R = H or alkyl) to an unsaturated metal atom occurs in two steps, with an intermediate containing a three-center electronic interaction.[31] A similar two-step reaction can be envisaged for the Si–Si bond in $CpFe(CO)Si_2Me_5$ (eq 16).

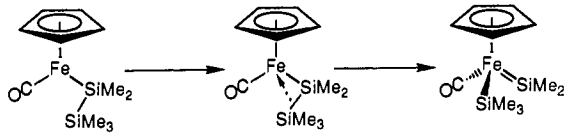

(16)

A potential energy barrier is predicted to exist between the intermediate species and the product in which oxidative addition is complete. Thus, in low-temperature matrices, the second step of the reaction does not occur, since the energy barrier is insurmountable. However, in solution, the reaction proceeds to give complete oxidative addition.

The reaction shown in eq 16 involves α-migration of an $SiMe_3$ group. Similar migrations involving cleavage of a C–C bond occur in the photoinduced ring expansion reactions of a number of Fp–cycloalkyl complexes (e.g., eq 17).[32] The products of these reactions (e.g., B) contain Fe—C and Fe=C bonds, resembling the silyl(silylene) structure proposed for X.

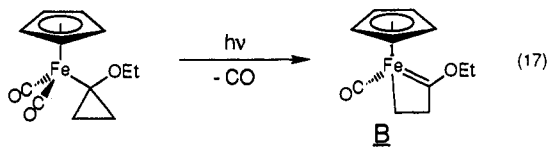

(17)

The photochemical reactions of other Fp–silanyl complexes are also known to result in Si–Si bond activation. For example, irradiation of $FpSi_3Me_7$ causes deoligomerization, yielding $FpSiMe_3$.[2,33] In this case there are two Si–Si linkages in the starting material. It is not clear whether activation of the α- or β-Si–Si bond occurs initially. When the Fp fragment is attached to a straight chain silanyl ligand with four or more silicon atoms, photolysis does not lead to deoligomerization. Instead rearrangement to give a branched chain silanyl ligand occurs, requiring both the breaking and reforming of Si–Si bonds.[33] These reactions are probably mediated by an unsaturated Fe center, formed on photodissociation of CO.

Photoinduced Si–Si bond activation has also been observed in $FpCH_2Si_2Me_5$.[1] Irradiation of this complex results in a skeletal

(30) (a) Traven, V. F.; West, R. *J. Am. Chem. Soc.* **1973**, *95*, 6824. (b) Sakurai, H.; Kira, M.; Uchida, T. *J. Am. Chem. Soc.* **1973**, *95*, 6826.

(31) Rabaa, H.; Saillard, J.-Y.; Schubert, U. *J. Organomet. Chem.* **1987**, *330*, 397.

(32) (a) Stenstrom, Y.; Jones, W. M. *Organometallics* **1986**, *5*, 178. (b) Conti, N. J.; Jones, W. M. *Organometallics* **1988**, *7*, 1669. (c) Conti, N. J.; Crowther, D. J.; Tivakornpannarai, S.; Jones, W. M. *Organometallics* **1990**, *9*, 175.

(33) Pannell, K. H.; Wang, L.-J.; Rozell, J. M. *Organometallics* **1989**, *8*, 550.

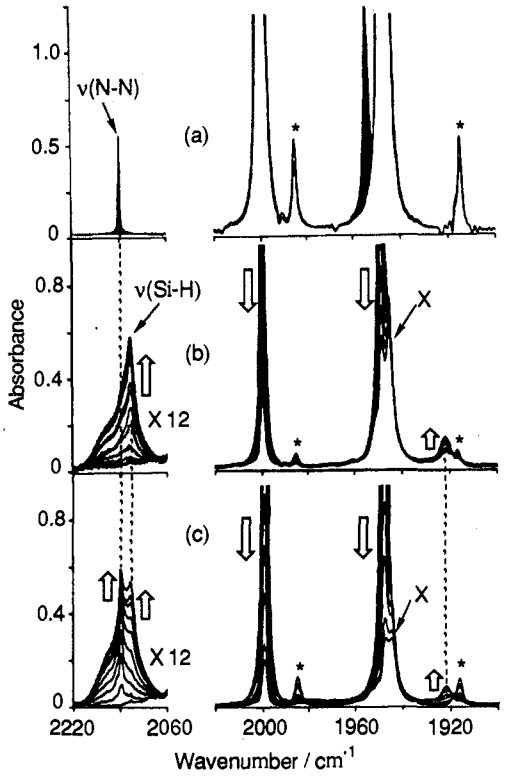

Figure 9. (a) Superimposed IR spectra obtained before and after 30-min irradiation (>325 nm) of $FpSiMe_3$ in liquid Xe at −100 °C under N_2 (150 psi). New absorptions due to $CpFe(CO)(N_2)SiMe_3$ are colored black. (b) IR spectra recorded during 7-min photolysis (>325 nm) of $FpSi_2Me_5$ in undoped liquid Xe at −100 °C. Note the production of bands due to $CpFe(CO)Si_2Me_5$, X, and a ν(Si–H) absorption. (c) IR spectra recorded during 13-min photolysis (>325 nm) of $FpSi_2Me_5$ in liquid Xe at −100 °C under N_2 (150 psi). Note the production of a weak ν(N–N) band in addition to the photoproduct absorptions in (b). Arrows indicate the behavior of individual absorptions during photolysis, and ^{13}CO satellites are marked with asterisks. The ν(Si–H) region is shown with an expanded absorbance scale in (b) and (c).

rearrangement of the disilanylmethyl ligand to give $FpSiMe_2CH_2SiMe_3$. No rearrangement was observed for $FpCH_2SiMe_3$, illustrating the significance of the presence of an Si–Si bond in the starting material. The behavior of $FpCH_2Si_2Me_5$ can be explained by the series of reactions shown in eq 18.

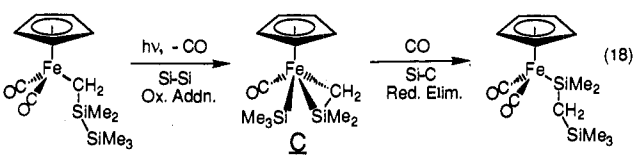

(18)

A similar reaction sequence, involving migrations of an H-atom rather than an $SiMe_3$ group, has been observed in the photoinduced conversion of $Fp^*CH_2SiMe_2H$ to Fp^*SiMe_3.[23] The intermediate species, C, in eq 18 can be formulated as either a metallasilacyclopropane or η^2-silene complex, a structure which has recently been identified by X-ray crystallography for $Cp^*Ru(PCy_3)(H)(CH_2SiPh_2)$.[34] The difference in structure of the proposed intermediates can explain why isomerization occurs for $FpCH_2Si_2Me_5$, whereas net loss of an $SiMe_2$ unit occurs for $FpSi_2Me_5$. Intramolecular reductive elimination of a relatively strong Si–C bond can occur for C, but no such route is available for X.

There are many other examples of intra- or intermolecular activation of Si–Si bonds by transition-metal fragments.[5] For instance, the photogenerated 16-electron species, $CpMn(CO)_2$, is implicated in the cleavage of organodisilanes.[35] There is also a recent report of the insertion of ethylene into the Si–Si bonds of organodisilanes, catalyzed by platinum–phosphine complexes.[36] Intermolecular oxidative addition of an Si–Si bond at a platinum center was confirmed as a key step in the catalytic cycle.

The Fate of the $SiMe_2$ Fragment. The second photochemical step in the deoligomerization of $FpSi_2Me_5$ is proposed to involve ejection of a silylene ($SiMe_2$) fragment from the intermediate species, X. In a study of the photochemistry of several base-stabilized transition-metal silylene complexes, Zybill et al. showed that irradiation can cause substitution of the SiR_2(base) unit by a phosphine ligand (e.g., eq 19).[37] There is, therefore, a precedent for the photochemical loss of an SiR_2 fragment from a transition-metal silylene complex.

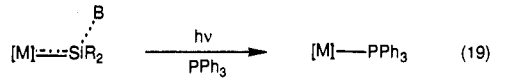

(19)

[M] = $Fe(CO)_3PPh_3$ or $Cr(CO)_4PPh_3$; B = $(Me_2N)_3PO$

Attempts to trap free silylene fragments in previous studies on the $FpSi_2R_5$ system proved unsuccessful.[2,3] Therefore, it appears that an SiR_2 moiety can be excluded from the iron complex without the production of free silylene in solution.

The isomerization of silylenes to give silenes is well established.[38] Dimethylsilylene can be generated photochemically in low-temperature matrices from the cyclohexasilane, $(Me_2Si)_6$.[39] On irradiation with visible light (450 nm), Me_2Si isomerizes to give 1-methylsilene, $Me(H)Si{=}CH_2$. Subsequent warming of the matrix leads to dimerization, forming 1,3-dimethyl-1,3-disilacyclobutane (eq 20).

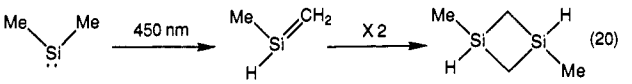

(20)

ν(Si-H) (Ar matrix): 2191, 2198 cm⁻¹ 2113, 2116, 2134 cm⁻¹

In the current study, deoligomerization was accompanied by the production of a broad IR band at 2121 cm^{-1}, which can be assigned as an Si–H stretching mode. This absorption occurs at a frequency between the three bands assigned to 1,3-dimethyl-1,3-disilacyclobutane in an argon matrix and might be due to the same dimeric compound. It is possible that dimethylsilylene might isomerize while in the excited state, immediately after ejection from X. This provides a plausible explanation for the inability to capture free Me_2Si with trapping reagents. However, we did not obtain any other evidence for the identity of this silicon-containing species.

Conclusions

The principal new finding of this study is that two distinct photochemical processes occur during the deoligomerization of $FpSi_2Me_5$. The first step is photodissociation of CO. Reaction of the 16-electron fragment with CO or other ligands is prevented by an interaction between the disilanyl ligand and the vacant coordination site. In solution, the primary photoproduct undergoes an intramolecular reaction, rationalized as oxidative addition of the Si–Si bond to the unsaturated Fe atom. This results in formation of a silyl(silylene)–iron complex, X, which is thermally stable in room temperature solution. The second photochemical step involves ejection of dimethylsilylene from this intermediate. It is thought that the $SiMe_2$ fragment gives rise to a product containing Si–H bond(s). Coordination of CO or another two-electron donor ligand completes the reaction, giving a mono-

(34) Campion, B. K.; Heyn, R. H.; Tilley, T. D. *J. Am. Chem. Soc.* **1988**, *110*, 7558.

(35) Schubert, U.; Rengstl, A. *J. Organomet. Chem.* **1979**, *170*, C37.

(36) Hayashi, T.; Kobayashi, T.; Kawamoto, A. M.; Yamashita, H.; Tanaka, M. *Organometallics* **1990**, *9*, 280.

(37) Zybill, C.; Wilkinson, D. L.; Leis, C.; Muller, G. *Angew. Chem., Int. Ed. Engl.* **1989**, *28*, 203.

(38) Brook, A. G.; Baines, K. M. *Adv. Organomet. Chem.* **1986**, *25*, 1.

(39) Drahnak, T. J.; Michl, J.; West, R. *J. Am. Chem. Soc.* **1981**, *103*, 1846.

silyl-iron complex, $CpFe(CO)(L)SiMe_3$ (L = CO, PPh_3, C_2H_4, or N_2).

Acknowledgment. We are grateful for support from the SERC, the EEC (Stimulation Contract No. SC1*0007), NATO (Grant No. 591/83), the Paul Instrument Fund of the Royal Society, the Donors of the Petroleum Research Fund, administered by the American Chemical Society, Perkin Elmer Ltd., and Nicolet Instruments Ltd. M.P. thanks the Nuffield Foundation for a Research Fellowship. We are also grateful to Dr. M. A. Healy, Mr. J. G. Gamble, Mr. J. M. Whalley, and Mr. D. Dye for their help and advice.

Application of Sensitivity Analysis to the Establishment of Intermolecular Potential Functions

Thomas S. Thacher,*,† A. T. Hagler,† and Herschel Rabitz‡

Contribution from Biosym Technologies, Inc., 10065 Barnes Canyon Road, San Diego, California 92121, and the Department of Chemistry, Princeton University, Princeton, New Jersey 08544. *Received February 20, 1990*

Abstract: The demands for accurate potential energy functions have increased synergistically with the sophistication and application of molecular modeling techniques. This study explored the utility of sensitivity analysis in the development and validation of potential energy functions. In particular, an intermolecular force field derived by fitting crystallographic data was examined using the methodology. The analysis was found to be very valuable in elucidating the relationship between the observables used in the fit and the resulting parameters. In addition, the method is shown to be useful as a quantitative probe for locating inaccuracies in the derived potential field.

The most common empirical methods for determining intermolecular potential energy expressions have proceeded in either a direct or an indirect manner.[1-6] In both methods the difference between a set of data and a corresponding set of values, calculated with use of an analytical expression for the intermolecular potential energy, is minimized by varying the potential parameters. The direct method involves generating a number of "data" points by performing ab initio calculations on a pair of molecules at different configurations. The "data" points usually considered are the intermolecular energies and the derivatives of the energy with respect to the atomic coordinates. In the indirect method the potential parameters are optimized to fit experimental crystal properties. While this approach is more satisfying than the former because the experimental potential surface is reproduced, the fitted points are restricted by the experimental geometry. This limitation is compounded by the symmetry of the crystal, which further constrains the region sampled on the potential energy surface. Additionally, many of the properties used in the optimization are a consequence of a summation over all different molecular interactions in the crystal. For example, the sublimation energy is found by summing over all the interactions between a central molecule and all other molecules within a given cutoff range. Thus, a least-squares fit to this observable reproduces the sum but not each individual interaction between the molecule and its neighbors. Because of this, it is important to simultaneously fit a variety of properties from crystals having different packing structures to ensure that the potential surface is adequately sampled.

In contrast to the indirect approach, the direct method requires a point-for-point fit of the data for each interaction geometry used in the optimization. Thus, it is more demanding that the indirect method and, as a result, the optimized parameters should be more defined. Unfortunately, the approach cannot always be applied because of limitations on computational time and the expense of generating the ab initio "data" points. Recently, efforts to develop methods to overcome this have been made. One method has been to replace the full calculations by calculations involving one molecule and a probe atom or diatom.[7] The other method has been to use the derivatives as "data".[8] The first method reduces the size of the calculation while the second reduces the number of calculations by using more information per calculation. Both approaches alleviate the computational problem somewhat and allow the approach to be used on larger systems. Nevertheless, the underlying problem, which is the lack of prior knowledge of where to calculate the "data" points to define the analytic function effectively with the fewest number of calculations, is not addressed.

This issue is related to a similar problem with the indirect method; that is, the relationship between the derived potential parameters and the crystal properties used in the optimization must be understood in order to efficiently define an analytic expression for the intermolecular potential. This study is part of an ongoing effort to systematically elucidate this relationship by using sensitivity analysis. This analysis has been shown to be useful for a wide variety of modeling problems in a number of different systems.[9-11] While the specifics of the application of sensitivity analysis to each of these problems differ, the common objective of the analysis is to use the technique to probe the dependence of the output on either the input or the mechanism that transforms the input into the output. When experimental data are used to optimize potential energy functions, the former objective is desired and the relevant quantities are the parametric sensitivity coefficients that quantify the sensitivity of the output to changes in the input parameters. In addition to the parametric coefficients, functional sensitivities are also of interest to determine the role of the *form* of the potential energy function in the optimization.

† Biosym Technologies, Inc.
‡ Princeton University.

(1) Pertsin, A. J.; Kitaigorodsky, A. I. *The Atom-Atom Potential Method: Application to Organic Molecular Solids*; Springer-Verlag: Berlin, 1987; Chapter 3.3, p 79.
(2) Miwa, Y.; Machida, K. *J. Am. Chem. Soc.* **1988**, *110*, 5183-5189.
(3) Bohm, H. J.; Ahlrichs, R.; Scharf, P.; Schiffer, H. *J. Chem. Phys.* **1984**, *81*, 1389-1395.
(4) Smit, P. H.; Derissen, J. L.; Van Duijneveldt, F. B. *Mol. Phys.* **1979**, *37*, 501-519.
(5) Williams, D. E.; Cox, S. R. *Acta Crystallogr.* **1984**, *B40*, 404-417.
(6) Warshel, A.; Lifson, S. *J. Chem. Phys.* **1970**, *53*, 582-594.
(7) Dinur, U.; Hagler, A. T. *J. Am. Chem. Soc.* **1989**, *111*, 5149-5151.
(8) Maple, J. R.; Dinur, U.; Hagler, A. T. *Proc. Natl. Acad. Sci. U.S.A.* **1988**, *85*, 5350-5354.
(9) Rabitz, H. *Comput. Chem.* **1981**, *5*, 267-180.
(10) Rabitz, H. *Chem. Rev.* **1987**, *87*, 101-112.
(11) Rabitz, H. *Science* **1989**, *246*, 221.

0002-7863/91/1513-2020$02.50/0